Hindawi Publishing Corporation
Journal of Nanomaterials
Volume 2016, Article ID 7135852, 15 pages
http://dx.doi.org/10.1155/2016/7135852

Research Article

Enhancement of the Antibacterial Activity of Silver Nanoparticles against Phytopathogenic Bacterium *Ralstonia solanacearum* by Stabilization

Juanni Chen, Shili Li, Jinxiang Luo, Rongsheng Wang, and Wei Ding

Laboratory of Natural Product Pesticide, College of Plant Protection, Southwest University, Chongqing 400715, China

Correspondence should be addressed to Wei Ding; dwing818@163.com

Received 16 December 2015; Revised 5 April 2016; Accepted 5 May 2016

Academic Editor: Piersandro Pallavicini

In this paper, the enhanced antibacterial activity of silver nanoparticles (AgNPs) against the phytopathogenic bacterium *Ralstonia solanacearum* after stabilization using selected surfactants (SDS, SDBS, TX-100, and Tween 80) was examined, in comparison with silver ion. Tween 80 was found to be the most preferable stabilizer of AgNPs due to the beneficial synergistic effects of the AgNPs and surfactant. However, all the surfactants nearly had no effects on the antibacterial activity of Ag^+. *In vitro*, Tween 80-stabilized AgNPs showed the highest bactericidal activity against *R. solanacearum*. Further measurements using TEM, fluorescence microscopy, and sodium dodecyl sulfate-polyacrylamide gel electrophoresis (SDS-PAGE) revealed that though Ag^+ and Tween 80-Ag^+ induced high toxicity, Tween 80-stabilized AgNPs displayed most severe damage when in direct contact with cells, causing mechanistic injury to the cell membrane and strongly modifying and destructing the cellular proteins. Meanwhile, *in vivo*, the pot experiments data indicated that the control efficiency of Tween 80-stabilized AgNPs on tobacco bacterial wilt was 96.71%, 90.11%, and 84.21%, at 7 days, 14 days, and 21 days, respectively. Based on the results evidencing their advantageous low dosage requirements and strong antimicrobial activity, Tween 80-stabilized AgNPs are a promising antibacterial agent for use in alternative crop disease control approaches.

1. Introduction

As an important economical crop, tobacco (*Nicotiana tabacum* L.) has been grown for thousands of years and cultivated worldwide [1]. However, bacterial wilt disease, caused by the phytopathogenic bacterium *Ralstonia solanacearum* (*R. solanacearum*), is prevalent in tropical regions with temperatures above 30°C and has long caused significant losses in tobacco production every year [2] and has been one of the most widespread and disastrous agricultural diseases, which infects various plant species, including a large number of agricultural crop plants and native trees [3]. The soilborne pathogen *R. solanacearum* initially invades crop-injured roots, particularly lateral roots, and spreads along the entire vascular system of the host plant through bacterial colonization in the crown and stem, inducing wilt symptoms [3]. Studies have shown that major virulence factors, such as polysaccharides and secreted proteins, greatly contribute to the pathogenesis of bacterial wilt disease [4].

Today, one of the most promising strategies for controlling bacterial wilt includes the breeding of resistant tobacco lines combined with improved cultural practices [2]. Previous studies have identified several genes governing resistance to bacterial wilt in tomato [5]. The Laurent group recently identified RRS1-R, a gene conferring broad-spectrum resistance to *R. solanacearum* and encoding a novel R protein [6]. Meanwhile, crop rotation using maize, soybean, sugarcane, and rice has been extensively applied to reduce the incidence of bacterial wilt in groundnut crops in China [7, 8]. However, the efficiency of this process is highly variable because of the numerous factors on which it depends, such as the viability and population of local bacterial strains [8]. Thus, innovative approaches are required to overcome these problems, and there is an urgent need for a focus on promising new technology, such as nanotechnology.

Nanotechnology employs nanomaterials, typically with particle sizes less than 100 nm in at least one dimension, and has promising applications in medical science and material

science because of the size-dependent qualities, high surface-to-volume ratio, and unique optical and physiochemical properties of these particles [9]. Previous studies have identified potential uses of nanotechnology in practically every field of agriculture, including the controlled release of fertilizers and micronutrients [10], pesticide degradation [11], biopesticide stabilization [12], nanosensing of plant pathogens and pesticides [13, 14], and soil conservation and remediation [15]. Nevertheless, nanotechnology-based antibacterial agents for agriculture applications remain in the margins of academic research. Possessing excellent antibacterial activity, silver nanoparticles (AgNPs) strongly inactivate a variety of bacterial pathogens (Gram-positive and Gram-negative) [16], fungal pathogens [17, 18], and viruses [19] and have been exploited for biomedical and environmental management applications [20, 21]. The release of silver ion (Ag^+) from their surface can be one of the significant reasons for their high antimicrobial activity. Most of the Ag^+ release occurs from oxidation of metallic nanosilver by dissolved oxygen and protons [22]. Much less information is available for plant pathogens, but several studies have attempted to develop nanomaterials, such as TiO_2, as antibacterial and antifungal tools for crop disease control [20]. Moreover, AgNPs have been utilized as a novel nanopesticide in research studies and have been efficiently employed to control agricultural plant diseases [21–23]. Notably, the most common application problem involves the agglomeration and diffusion of these nanoparticles, which reduce antibacterial activity. Thus, studies have used various organic [24] and inorganic substances [25] as well as powerful carriers [26] to stabilize AgNPs. These substances can strongly influence the antibacterial activity and reduce the biological toxicity of nanoparticles. Except for the discharge of Ag^+, the toxicity of AgNPs is highly dependent on their size [27], shape [28], surface chemistry [29], stability, and surface charge [10]. Previous studies have focused on the positive effects of stabilizers, including sodium dodecyl sulfate (SDS), polyoxyethylene sorbitan monooleate (Tween 80), cetyltrimethylammonium bromide (CTAB), and polyvinylpyrrolidone (PVP), on the toxicity of AgNPs, particularly when modified by SDS, for which the minimum inhibition concentration (MIC) was reduced below the "magic value" of 1 μg/mL [10]. This is because their surface charge and molecular structure are considered to be the dominant factor in changing the surface chemistry of AgNPs. Additionally, Panáček et al. showed that SDS-capped silver nanoparticles at concentrations as low as 0.05 mg/L displayed better antifungal activity than silver nanoparticles alone [17]. Nonetheless, the toxicity of stabilized AgNPs also depends on the bacterial strain, and the detailed toxicity mechanisms of AgNPs against phytopathogenic bacteria remain elusive. Therefore, it is significant to investigate the antibacterial activity of stabilized AgNPs, thereby paving the way toward the development of a broader and novel measurement to plant management.

Herein, we used the phytopathogenic bacteria *R. solanacearum*, causing far-reaching catastrophic diseases in tobacco and most other cultivated crops, as a platform to investigate the antibacterial activity of silver nanoparticles and screen suitable stabilizers for the enhancement of the antibacterial action of AgNPs. Intense efforts have been devoted to comparing the antibacterial activities of pure AgNPs with those of AgNPs stabilized using selected surfactants agents, including SDS, sodium dodecylbenzenesulfonate (SDBS), octylphenol polyethoxylate (TX-100), and polysorbate 80 (Tween 80). Ag^+ was used to be compared with the antibacterial activity. The results demonstrated that the surfactant Tween 80 was the most effective for improving the toxicity of AgNPs. Specifically, the high bacteriostatic and bactericidal activities of AgNPs against *R. solanacearum in vitro* were examined and the underlying toxicity mechanisms were investigated by TEM, fluorescence microscopy, and SDS-PAGE. Further, this study focuses on the practical application of Tween 80-stabilized AgNPs for controlling tobacco bacterial wilt *in vivo*.

2. Materials and Methods

2.1. Chemicals and Apparatus. Silver nitrate ($AgNO_3$), 1% sodium citrate dihydrate, and sodium borohydride ($NaBH_4$) were obtained from Sangon Biotech (Chongqing) Co., Ltd. All the surfactants, including SDS, SDBS, TX-100, and Tween 80, were purchased from Sigma-Aldrich. Additional chemicals were purchased from Sangon Biotech (Chongqing) Co., Ltd. All solutions were made using sterile Milli-Q (mQ) water. Several instruments were used to characterize and analyze the physical and chemical properties of AgNPs samples, including transmission electron microscope (TEM, JEM-2100, Japan). The ultraviolet absorption spectra were acquired on the Nicolet Evolution 300 UV-Vis spectrometer. The particle size distribution and zeta potential of all AgNPs dispersions were evaluated on Malvern Zetasizer Nano Series (Malvern, UK). Cell morphology was conducted on TEM (FEI, Czech Republic).

2.2. Synthesis of AgNPs Using the Chemical Reduction Method. AgNPs were prepared using a previously described procedure [30]. AgNPs were obtained after reducing $AgNO_3$ with $NaBH_4$ in a water suspension using citrate as a stabilizing agent. Briefly, 5 mL of 10 mM $AgNO_3$ was mixed with 45 mL of ultrapure water at 45°C and rapidly heated to boiling. Subsequently, 1 mL of 1% sodium citrate dihydrate and 300 μL of 3 mM $NaBH_4$ were injected dropwise under vigorous stirring, and the resulting solution was boiled for 60 min. After cooling under ambient conditions, the solution was filtered through a polycarbonate membrane (0.22 μm). The final mixture was centrifuged at 8000 rpm, precipitated, and lyophilized. Alternatively, the prepared AgNPs were further stabilized using the selected surfactants (SDS, SDBS, TX-100, and Tween 80) at a final concentration of 1% (w/w), and the pure and modified dispersed AgNPs were then serially diluted. The morphology was observed using TEM (JEM-2100, Japan) and average size of the prepared AgNPs was analyzed by dynamic light scatting (DLS) using Zetasizer Nano ZS (Malvern Instruments, England), respectively. The UV-Vis absorption spectra were recorded using a Shimadzu UV-1650PC spectrometer to characterize the AgNPs.

2.3. Silver Ion Release and Evaluation of the Stability of Bare and Stabilized AgNPs. The silver ion release concentration of prepared AgNPs was monitored by the inductively coupled plasma mass spectrometer (ICP-MS) (Thermo Scientific). Mainly, 1 mL of 10 mg/L AgNPs in Nutrient Broth (pH 7.0) at different times (0, 5, 10, 20, 60, and 120 min) was taken to be centrifuged at 9000 rpm for 40 min. After that, the supernatant continued to be filtered by Microcon centrifugal filters (3000 MWCO), made of regenerated cellulose. 100 μL of the final filtrates was added to 2% HNO_3 solution to make a total volume of 10 mL. Afterward, the samples were measured using inductively coupled plasma mass spectrometer (ICP-MS) (X Series 2, Thermo Scientific).

To understand the stability characteristics of AgNPs, experiments were performed to evaluate whether the surfactants improved the particle stability by influencing the surface charge and aggregation state. The zeta potentials were measured by Zetasizer Nano ZS mentioned above under different pH value via adjustment of the pH of the dispersions with HCl (acid region) or NaOH (basic region). We determined the particle diameter to study the effect of ion strength on the stability of nanoparticle. NaCl was mixed with bare and surfactants-stabilized AgNPs (pH 7.0) to maintain the ion strength at various concentrations (10, 50, 100, and 200 mM). After incubation for 16 min, particle diameter of nanoparticle was determined by the same instrument.

2.4. Bacterial Culture. *R. solanacearum* strains were provided from the Laboratory of Natural Product Pesticide of Southwest University (Chongqing, China). The separated *R. solanacearum* strains were cultured in Nutrient Broth (NB medium) containing 3.0 g/L beef extract, 1.0 g/L yeast extract, 5.0 g/L peptone, and 10.0 g/L glucose, pH 7.0, in a humidified incubator overnight at 30°C under constant agitation. The bacteria cultures were harvested at the mid-exponential growth phase and centrifuged at 6,000 rpm for 5 min to collect the cells. The bacterial pellet was then washed three times with deionized water to wash off the medium constituents and other chemical macromolecules. The cells were resuspended in deionized water, and the suspensions were diluted to 10^5~10^6 colony-forming units (CFU/mL) for experimental use.

2.5. Determination of the MIC and MBC. To investigate the antibacterial activity of the synthesized nanomaterials against phytopathogen, stabilized AgNPs were compared with pure AgNPs. The bacteriostatic and bactericidal activities of AgNPs against *R. solanacearum* were examined using a typical microdilution method (ISO 10932|IDF 223:2010) to determine the minimal inhibitory concentration (MIC) and minimal bactericidal concentration (MBC).

AgNPs were initially diluted to 78 mg/L in a NB medium. The dispersed AgNP stocks were then diluted with NB medium in a geometric progression from 2 to 2048 times to obtain concentrations ranging from 39 to 0.08 mg/L (39, 19.5, 9.76, 4.88, 2.44, 1.22, 0.61, 0.31, 0.15, and 0.08 mg/L). Next, 100 μL of the prepared bacterial suspension (~10^5 CFU/mL) was mixed with 100 μL of a series of diluted AgNPs in a 96-well ELISA plate. The final AgNP concentration range examined in the present study was between 39 and 0.04 mg/L. Namely, the AgNPs were modified with surfactants after serially diluting the initial concentration of 1% (w/w) to generate concentrations ranging from 0.5% to 9.76×10^{-4}% (w/w). As a positive control, 100 μL *R. solanacearum* was inoculated into the same volume of NB medium in the absence of nanoparticles, and 100 μL of pure broth mixed with same volume of nanoparticle served as a negative control. The inoculated plates were incubated at 30°C for 24 h with shaking (120 rpm), and the absorbance of each well was determined using an automatic ELISA microplate reader (Thermo Multiskan MK3, USA). The MIC value was defined as the lowest concentration of AgNPs at which the visible growth of microorganisms was significantly inhibited compared with the blank.

The viability of *R. solanacearum* cells mixed with AgNPs was determined after counting the standardized colony-forming units (CFU). Briefly, after incubating the inoculum suspensions (~10^5 CFU/mL) and nanoparticles for 24 h with shaking (120 rpm), gradient dilutions of each sample were transferred onto LB agar plates, cultured at 30°C for two days, and spotted until growth was observed on the control plates. Subsequently, the cell colonies were counted, and the lowest concentrations showing no growth or fewer than three colonies (approximately 99 to 99.5% killing activity) were recorded as the MBC. The cell mortality (% of the control) was expressed as (counts of the control – counts of the treated samples)/counts of the control. All treatments were individually repeated at least three times. Control experiments were also conducted in parallel. Similarly, surfactants were diluted with NB medium in a geometric progression from 2 to 2048 times to obtain concentrations ranging from 0.5% to 9.76×10^{-4}% (w/w). Given the major role played by the released Ag^+ ions in the antibacterial activity of AgNPs [31], as a comparison assay, we also measured the MIC and MBC of surfactants, Ag^+, and surfactants-modified Ag^+ using the same methods. $AgNO_3$ was used to supply the source of Ag^+. 1000 mg/L of $AgNO_3$ which contains 635 mg/L Ag^+ was mixed with surfactants to abstain the initial concentration of 1% (w/w), and as stated above, $AgNO_3$ was serially diluted in a geometric progression.

2.6. Inhibition of Bacterial Growth. The bacteria cells were grown in liquid medium, and the bacterial growth was measured using the same culture medium by comparing the growth in the presence and absence of each type of AgNP (pure AgNPs, Ag^+, and surfactant-stabilized AgNP dispersions) at different concentrations. The bacteria growth curve was generated as previously described [32]. Typically, 100 μL of the diluted cell suspensions (~10^5 CFU/mL) mixed with identical volumes of nanomaterials at different test concentrations (39, 19.5, 9.76, 4.88, 2.44, 1.22, 0.61, 0.31, 0.15, and 0.08 mg/L) was incubated at 30°C for 2 h with gentle shaking. The control sample contained 100 μL of the cell suspensions added to 100 μL of DI water. The mixture was then transferred to 5 mL tubes containing 2 mL of NB medium, and the tubes were incubated at 30°C for 24 h with shaking at 120 rpm. The bacterial cell density was measured at an optical density (OD) of 600 nm every two hours using

a Nicolet Evolution 300 UV-Vis spectrometer. All the samples were tested in triplicate, and the average value was calculated. The growth curves were plotted by the OD value at 600 nm versus growth time.

2.7. Cell Imaging Using TEM. The bacterial cells were exponentially collected and diluted to 4×10^8 colony-forming units (CFU)/mL. Subsequently, the cells were incubated with Tween 80 (8% w/w), Ag^+ (2.48 mg/L), AgNPs (19.5 mg/L), and Tween 80-stabilized AgNPs (1.22 mg/L) in the dark at 30°C for 3 h with shaking at 120 rpm. TEM was then used to observe the morphological changes of the bacteria as previously described [31]. After treatment and centrifugation at 6000 rpm, the condensed cells were fixed with 2.5% glutaraldehyde, postfixed with 1% aqueous OsO_4 (Fluka), and washed with 0.1 M phosphate buffer, pH 7.0. The samples were then dehydrated in an ascending ethanol series (30, 50, 70, 80, 90, and 100%) for 15 min and dried in a vacuum oven. Thin sections containing the cells were placed onto copper grids and observed under TEM (FEI, Czech Republic).

2.8. Cell Imaging Using Fluorescence Microscopy. Briefly, 1 mL of the bacterial suspension (10^7 to 10^8 CFU per mL) and 100 mL of 2.48 mg/L Ag^+, AgNPs (19.5 mg/L), and Tween 80-stabilized AgNPs (1.22 mg/L) were mixed in a centrifuge tube and incubated at 30°C for 2 h with gentle shaking. After harvesting via centrifugation at 6000 rpm, the bacteria were resuspended in 1 mL of water, and the cells were stained with 10 mL propidium iodide (PI, excitation/emission at 535 nm/617 nm; Sigma-Aldrich) for 15 min, followed by counterstaining with 10 mL 40-6-diamidino-2-phenylindole (DAPI, excitation/emission at 358 nm/461 nm; Sigma-Aldrich) for 5 min in the dark. As a control, the cells were incubated with deionized water. The test samples were then observed under an inverted fluorescence microscope (Eclipse Ti, Nikon). The cell death percentage was calculated as the ratio of the number of cells stained with PI (dead bacteria) to the number of cells stained with DAPI plus PI (total bacteria).

2.9. Protein Damage Assay. The protein damage in *R. solanacearum* cells incubated with AgNPs was investigated using SDS-PAGE as previously described [33]. *R. solanacearum* cells were collected at the exponential growth phase and diluted. We selected the final highest concentration to evaluate the damage of AgNPs to bacterial protein. Ag^+ (2.48 mg/L), Tween 80 (8% w/w), 19.5 mg/L of AgNPs, and 1.22 mg/L Tween 80-stabilized AgNPs were mixed with the bacterial suspension for 2 h, respectively, and cells treated with sterile deionized water were used as a control. Subsequently, all treated samples were boiled in water for 10 min, and 30 μL of bacteria suspension was mixed with 6 μL of 5x standard SDS-PAGE sample loading buffer. After centrifugation, the supernatants were loaded directly onto 10% precast polyacrylamide gels. Electrophoresis was performed on a Bio-Rad vertical electrophoresis system at 100 V for nearly 2 h.

2.10. A Pot Experiment. The control efficacy of Tween 80-stabilized AgNPs on tobacco bacterial wilt was examined *in vivo* by pot experiments. Four leaves old tobacco seedlings grown in pots were selected and 20 plants were prepared for each treatment. And 30 mL of diluted Tween 80-stabilized AgNPs suspension (1.22 mg/L) was evenly irrigated into tobacco roots. A blank control sample was treated with sterile water in this experiment. These pots were arranged randomly with three replicates per treatment. Twelve hours later, *R. solanacearum* was inoculated via noninjured root inoculation at OD600 = 0.1 ($\approx 10^7$ CFU/mL) per plant. The inoculated tobacco seedlings were cultivated in a plant growth chamber at the temperature of 30 ± 1°C, relative humidity of 85–90%, and light period of 14 h. Following the inoculation of *R. solanacearum*, the disease occurrence and disease index every 2 d from the first observation of bacterial wilt diseased plants were monitored until all of the control plants had almost withered. The disease incidence, disease index, and control efficacy were calculated at a period of 7 d, 14 d, and 21 d.

3. Results and Discussion

3.1. Dispersibility and Morphology Dispersibility. The morphology and aggregation of Ag nanoparticles prepared using the chemical reduction method were examined using TEM (JEM-2100, Japan). As shown in Figure 1(a), the synthesized silver nanoparticles were nearly spherical, and aggregates ranging from 10 nm to 100 nm in size were observed. After stabilization with the four surfactants, AgNPs seem to display better dispersibility. A comparison with the size distribution between the uncapped and stabilized AgNPs was further analyzed by DLS. The results showed that particles with small size (<10 nm) were slighter in the presence of surfactants than pristine AgNPs, but the differences were not significant (Figure 1(a)). These small particles may be fragmented from larger spherical particles due to partial dissolution and recrystallization [34]. It would be indicated that there is no change in morphology or aggregation. In addition, the nanoparticles were characterized using UV-visible spectroscopy, one of the most widely used techniques for the structural characterization of nanomaterials. The results revealed a maximum absorption peak at approximately a wavelength of 410 nm, consistent with the reported characteristic of the surface plasmon absorption band of silver nanoparticles (see Figure S1 in Supplementary Material available online at http://dx.doi.org/10.1155/2016/7135852). But, for stabilized AgNPs, there was slight red shift of the absorption band indicating the presence of an oxidized layer on the AgNPs particle surface [35, 36].

3.2. Silver Ion Release from Bare AgNPs and Stabilized AgNPs. AgNPs can leach silver ion (Ag^+) due to the oxidation of metallic nanosilver by dissolved oxygen and protons, which is an important factor to value their fate, transport, and biological interaction [36]. Silver ion was greatly in charge of the high antibacterial activity of AgNPs [37]. In this experiment, Ag^+ release kinetics of bare AgNPs and stabilized AgNPs in NB medium were monitored electrochemically and analyzed using ICP-MS technology. According to Figure 2(a),

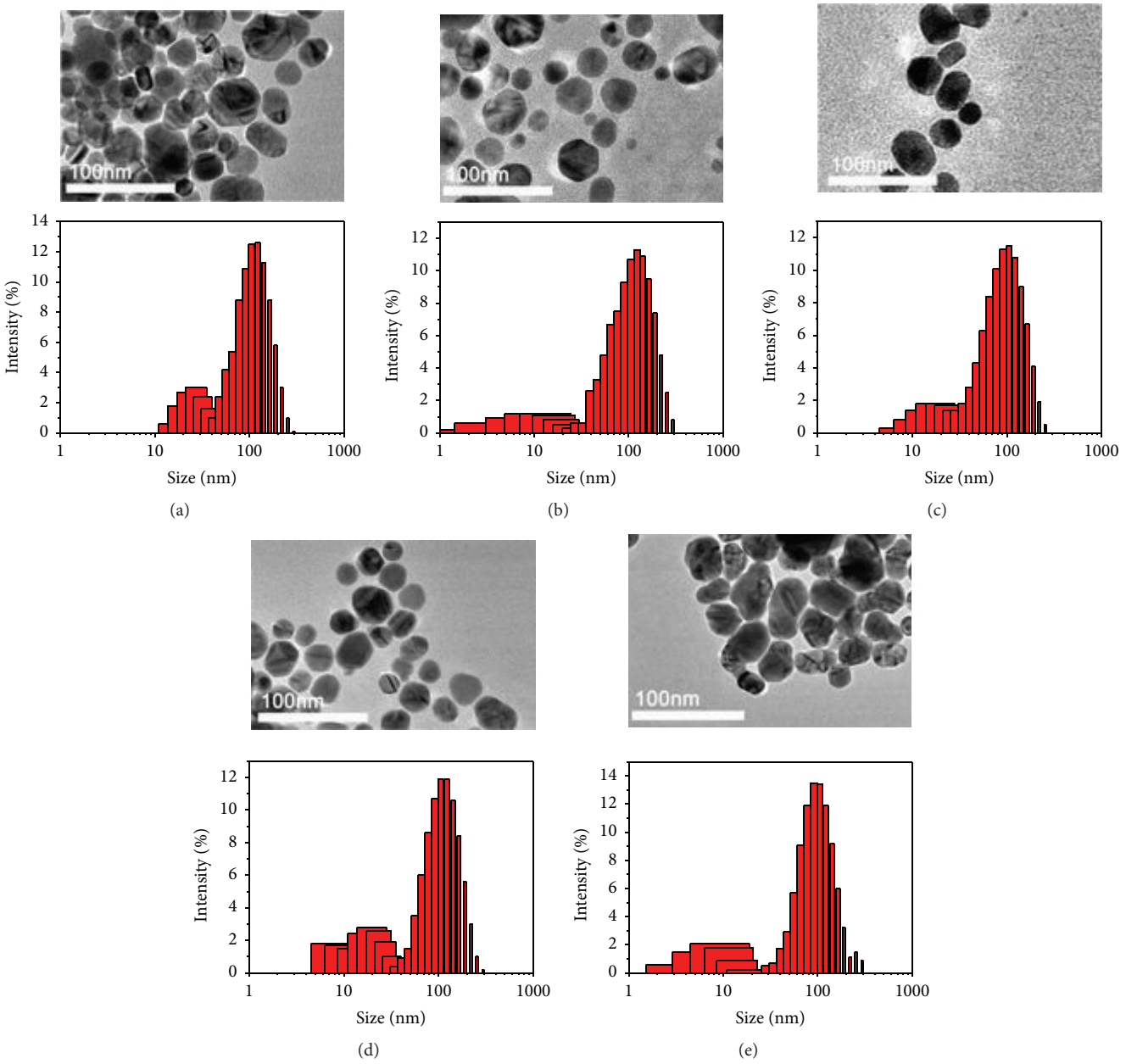

Figure 1: Transmission electron images of bare AgNP (a), SDS-AgNPs (b), SDBS-AgNPs (c), TX-100-AgNPs (d), and Tween 80-AgNPs (e) in water and their corresponding particles size distribution histogram. Note that the acronyms SDS, SDBS, TX-100, and Tween 80 indicate sodium dodecyl sulfate, sodium dodecyl benzene sulfonate, Triton X-100, and polysorbate 80, respectively.

unstabilized AgNPs rapidly discharged high concentration silver ions within 20 min, and the content nearly reached saturation (38.2 μg/mL) 20 min. The reason for silver ion discharge involves the presence of an oxide layer on the nanosilver surface [36, 38]. For stabilized AgNPs, the initial dissolution was more slightly prompt, as soon as, however, the slowly ascending discharge occurs, and the Ag^+ hardly uncharged. It can be noted that the presence of the surfactants induced subdued dissolution of silver ion from AgNPs and the content of the released Ag^+ decreased were consistently less than bare AgNPs, especially Tween 80-stabilized nanosilver, Ag^+ from which is rather minimal, reduced by 50% in comparison with bare AgNPs.

3.3. Effects of pH Value and Ionic Strength on the AgNPs Stability. To evaluate the stability of surfactants-modified AgNPs, we investigated the zeta potential and particle diameter under different pH value and ionic strength. As we know, AgNPs possess extremely high surface charged densities [35]. Stabilizer agents can usually change the surface charge and hinder the nanoparticle aggregation process by enhancing electrostatic or steric repulsion interaction, thereby improving the stability of the nanoparticle suspension [31, 38]. Generally, zeta potentials greater than +30 mV or less than −30 mV are considered strongly to be stable. It can be seen from Figure 2(b) that bare AgNPs exhibited an obvious decline in zeta potential when the pH value of solution ranged

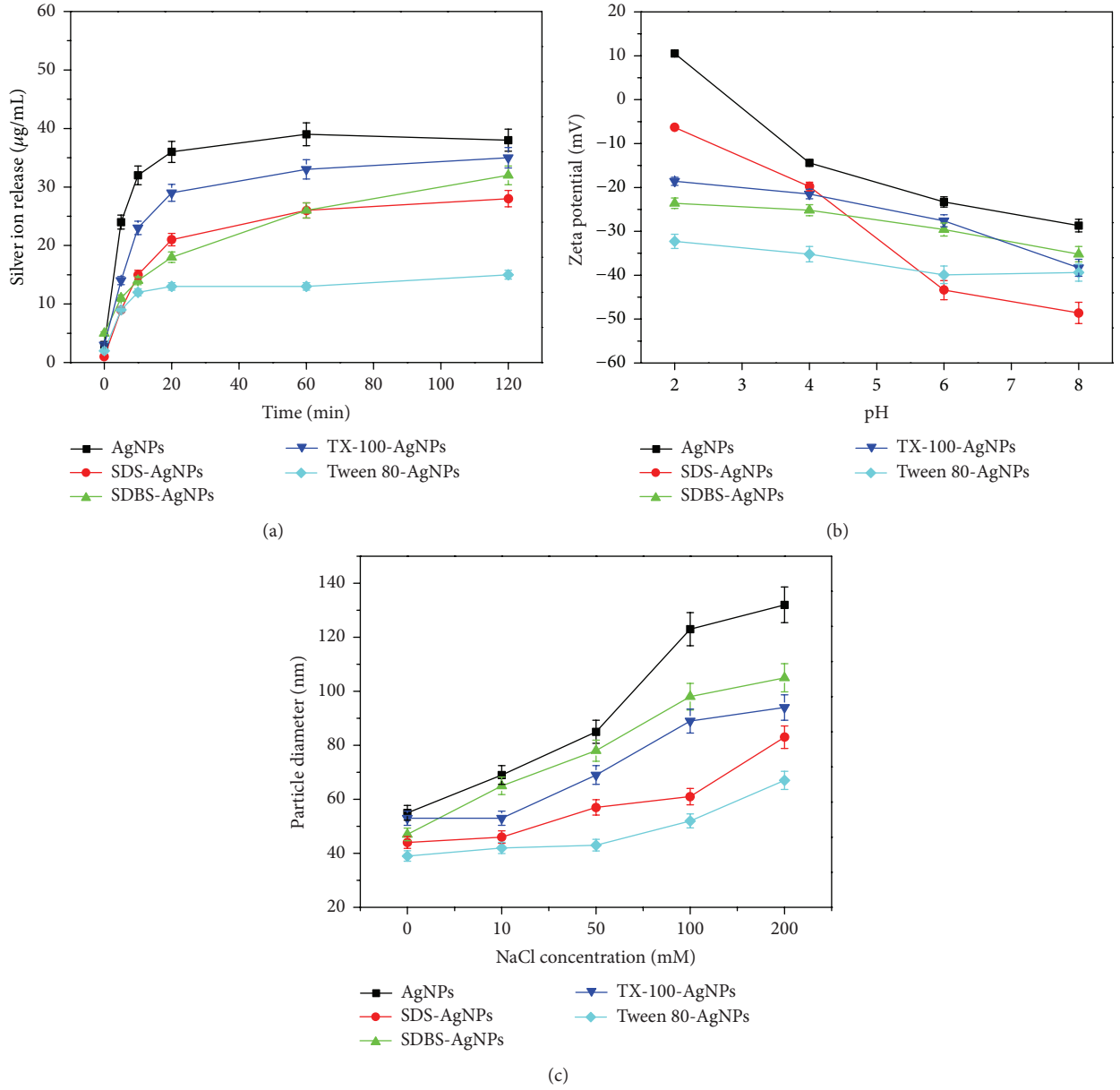

Figure 2: Release of silver ion from bare AgNPs and surfactants-stabilized AgNPs (a) and the effect of different pH on the measured zeta potential (b) and the effect of ionic strength on the particle diameter (c) under pH 6.8 in the presence of 100 mM NaCl.

from 2 to 8, displaying small value. SDS induced a rapid decline in the surface charge of AgNPs, but zeta potentials were moderately decreased with the increasing pH value in the presence of SDBS and TX-100. The zeta potential was fluctuated at −30 mV. Following the DLVO theory, the strong stability effects were observed because the absolute value of the surface charge reflected in the nearly doubled value of zeta potential was significantly increased. However, changes in solution pH had nearly no effect on the electric potential of sterically stabilized Tween 80-stabilized AgNPs, the average of which was −36.7 mV in the pH variation range, persistently being the stabilizing force for AgNPs.

Further, we assessed the AgNPs stability by motioning the aggregation kinetics of nanoparticles in sodium chloride (NaCl) solution. It could be noted that, in the presence of electrolyte solution (NaCl), sliver chloride (AgCl) deposits possibly are developed on the surface of or around the nanoparticle, on account of the interaction between chloridion (Cl^-) and the Ag^+ released from the dissolving uncapped silver nanoparticle [35]. Our results in this experiment showed that SDS- and SDBS-modified AgNPs exhibited a slighter decrease in the aggregation particle diameter than that of pure AgNPs under the highest NaCl concentration (200 mM), with the value equal to 83.2 nm and 105.5 nm, respectively. Differently, there was almost little change after stabilizing with Tween 80 under systems with different NaCl concentration and pH 7.0 within previous 16 min (Figure 2(b)), implying the nearly instantaneous

Table 1: The minimum inhibitory concentration and minimum bactericidal concentration of pure surfactants, Ag^+, and AgNPs with and without surfactants toward *R. solanacearum*.

Dispersions	MIC, mg/L (%)	MBC, mg/L (%)
SDS	0.125%	0.5%
SDBS	0.0625%	0.125%
TX-100	2%	4%
Tween 80	8%	>16%
Ag^+	1.24 mg/L	2.48 mg/L
Ag^+ + SDS	1.24 (0.2×10^{-3}%)	2.48 (0.39×10^{-2}%)
Ag^+ + SDBS	1.24 (0.2×10^{-3}%)	2.48 (0.39×10^{-2}%)
Ag^+ + TX-100	1.24 (0.2×10^{-2}%)	2.48 (0.39×10^{-2}%)
Ag^+ + Tween 80	1.24 (0.2×10^{-3}%)	2.48 (0.39×10^{-2}%)
AgNPs	4.88 mg/L	19.5 mg/L
AgNPs + SDBS	1.22 (1.56×10^{-2}%)	4.88 (6.25×10^{-2}%)
AgNPs + SDS	1.22 (1.56×10^{-2}%)	4.88 (6.25×10^{-2}%)
AgNPs + TX-100	4.88 (6.25×10^{-2}%)	19.5 (0.25%)
AgNPs + Tween 80	0.61 (0.78×10^{-2}%)	1.22 (1.56×10^{-2}%)

Notice that the results were repeated at least in triplicate.

sterical stabilization for AgNPs by the protective Tween 80 layer. Further, the phenomenon greatly associated with the strong prevention of Ag^+ dissolution and particle aggregates (Figure 2(c)). This is because the less Ag^+ released from AgNPs may be sorbed on their surface and induced the less formation of AgCl sedimentation [38].

Above all, all the surfactants seem to enhance the nanoparticle's stability. However, it is worth mentioning that Tween 80 tremendously plays a more important role than other agents like SDS and SDBS in stability of the AgNPs dispersion by forming low zeta potential and preventing particle aggregates. Li et al. also demonstrated that the SDS and Tween coating can consistently reduce the initial particle sizes of capped AgNPs across the entire range of NaCl concentrations due to blocking particle dissolution process [35]. Similar to the previous results, the nonionic surfactant Tween 80 performed sterically repulsive interactions by the way of formation of thicker and denser coating layers compared with electrosteric repulsion of anion SDS, thus inducing the improvement of nanoparticle stability more than other agents [31, 39], being consistent with our results.

3.4. Bacteriostatic and Bactericidal Activity of the Pure and Surfactant-Stabilized AgNPs. In this experiment, a phytopathogenic strain of *R. solanacearum*, which causes severe bacterial wilt in tobacco, was used to investigate the bacteriostatic and bactericidal activity of pure and surfactant-stabilized AgNPs. The MIC and MBC were determined using the microdilution method. As shown in Table 1, the surfactants affected the antibacterial activity of AgNPs toward *R. solanacearum* to different extents. Specifically, the antibacterial action of pure AgNPs was evidently enhanced upon dispersion in these surfactants. Among the four stabilizing agents, Tween 80 was the most effective, yielding a MIC of AgNPs (0.61 mg/L, an extremely low value) that was 8-fold lower than the value of pure AgNPs (up to 4.88 mg/L). The antibacterial activity of AgNPs was 4-fold higher in both SDBS and SDS, displaying identical minimal inhibition concentration values of 1.22 mg/L. In contrast, after stabilization with TX-100, no changes in the bacteriostatic action of this nanoparticle were observed, with the same value for both MIC and MBC.

We also assessed the bactericidal activity of the various AgNP dispersions. The colony-forming units (CFU) method was used to further verify the mortality of *R. solanacearum* cells from the growing cells in the presence of different concentrations of suspensions. Notably, all the surfactants tested in the present study significantly decreased the MBC of AgNPs, particularly Tween 80. Consistent with a previous study, pure AgNPs, without the introduction of any surfactant, showed a high-intensity lethal effect at a high dose of 19.5 mg/L. Surprisingly, the MBC of Tween 80-stabilized AgNPs was 1.22 mg/L, which is lower than that of pure AgNPs. In comparison, 2.48 mg/L of Ag^+ and 2.48 mg/L of Tween 80-Ag^+ induced a complete death of bacteria, respectively (Table 1). As for Tween 80-stabilized AgNPs, it contains 0.46 μg/mL of Ag^+ when at the lethal concentration. It means that Tween 80-stabilized AgNPs make better toxicity effects than Tween 80-stabilized $AgNO_3$. And we concluded the fact that the high antibacterial activity of Tween 80-stabilized AgNPs is obviously associated with the released silver ion, as stated in previous study [40], but, for another, it is attributed to not only the presence of silver ion but also the AgNPs. Thus, Tween 80 provided the greatest increase in the antibacterial activity of silver nanoparticles, improving the toxicity efficiency by 16-fold. The extraordinary improvement of antibacterial activity of AgNPs by Tween 80 is supposedly connected with the strong steric stabilization effect, causing the formation of weak interaction among nanoparticle assemblies, although Tween 80 had slight effect on the surface charge of AgNPs (Figure 2) [31].

SDS and SDBS exhibited similar effects on the antibacterial activity of AgNPs, both with an MBC of 4.88 mg/L, at which complete bactericidal activity was observed. Indeed, both surfactants enhanced the antibacterial activity of AgNPs fourfold. The results have strong relations with the better

stability of the silver NPs modified by anionic surfactants, SDS and SDBS. Based on the research, the stabilizing effect was connected to the electrostatic stabilization, inducing dramatic increase of the surface charge of AgNPs, the potential value of which is approximately double that of unmodified AgNPs (Figure 2). For another, the proposed steric effect of the hydrophilic and hydrophobic groups of the surfactant molecules should also be taken into account [41]. In contrast, the MBC of AgNPs in the presence of TX-100 was 19.5 mg/L, demonstrating that TX-100 had no effect on the antibacterial activity of AgNPs.

On the other hand, to investigate the relationship between AgNPs toxicity and the use of surfactants, we conducted another antibacterial experiment using surfactants alone. The results suggested that the application of surfactants-stabilized AgNPs not only increased the antibacterial activity of AgNPs against *R. solanacearum*, with the exception of TX-100, but also enhanced the activities of the surfactants (Table 1). Notably, a synergistic effect of the stabilizers and AgNPs on the antibacterial activity was observed. The interaction efficiency differed by surfactant. As shown in Table 1, pure SDS indicated inhibitory and completely lethal effects of *R. solanacearum* at a treatment concentration of 0.125% and 0.5% (w/w), respectively, just as shown in the growth curve (Figure S2A). However, the SDS-stabilized AgNPs exhibited bactericidal effects at a concentration of 4.88 mg/L, in which the SDS content was only equal to 0.0625% (w/w), a much lower dosage than that of pure SDS solution. Thus, the concentration of SDS-stabilized AgNPs needed to induce a lethal effect on bacteria was 4 and 2.5 times lower than that of pure SDS and pure AgNPs, respectively. Previous studies have also confirmed that SDS-stabilized AgNPs exhibited even higher fungicidal activity than pure AgNPs [17]. Similarly, SDBS and TX-100 solution absolutely induced no growth of *R. solanacearum* under the concentration of 0.125% (w/w) and 4% (w/w), respectively (Figure S2 and Table 1). In the case of bacteria killing with SDBS- and TX-100-stabilized nanoparticles, the concentration of SDBS decreased from 0.125% to 0.0625% (w/w) and the concentration of SDBS decreased from 4% to 0.25% (w/w). Significantly, higher antibacterial activity was observed for Tween 80-stabilized AgNPs (1.22 mg/L), which contained only 0.0156% (w/w) Tween 80. In fact, however, as shown in Figure S2D and Table 1, the MIC and MBC of Tween 80 were 8% and above 16%. Although pure Tween 80 exhibited an inhibitory effect, it did not provide complete bactericidal action. According to the above results, surfactant-stabilized nanoparticles strengthened the toxicity of surfactants against *R. solanacearum*. However, it seems that application of surfactants had no change on the antibacterial activity of $AgNO_3$, possibly because the Ag^+ itself induced strong toxicity, and the surfactant concentrations in $AgNO_3$ solution under MIC and MBC of mixture were not high enough to exert antibacterial activity (Table 1).

3.5. Effects of Pure and Surfactant-Stabilized AgNPs on Bacterial Growth. The growth inhibitory effect of AgNPs stabilized with four surfactant agents (SDS, SDBS, TX-100, and Tween 80) against the tobacco bacterial wilt pathogen *R. solanacearum* was evaluated in detail by measuring the bacterial growth curves. The bacterial logarithmic growth kinetics was monitored in NB medium (initial bacterial concentration, ~10^5 CFU/mL) after incubation with different concentrations of pure and stabilized silver nanoparticles.

As shown in Figure 3, AgNPs inhibited bacterial growth in the presence and absence of surfactants over the wide range of concentrations assayed, and the growth inhibition rate of the tested bacteria depended strongly on the surfactant concentration and type. To obtain clearer results from the bacterial growth curves, only five different representative AgNPs concentrations were examined in the present study. The results showed that surfactant-stabilized AgNPs showed a stronger inhibition effect on the growth of *R. solanacearum* than did pure AgNPs. It is evident from Figure 3(a) that when treated with SDS and SDBS-stabilized AgNPs at a concentration of 4.88 mg/L, the *R. solanacearum* growth inhibition was much faster than that after treatment with the same concentration of pure AgNPs. In particular, Tween 80-stabilized AgNPs exhibited the strongest and most efficient growth inhibition at concentrations ranging from 0.15 to 1.22 mg/L. As shown in Figures 3(a)–3(e), at a representative concentration of 1.22 mg/L, all surfactant-stabilized AgNPs showed a much stronger inhibitory effect on bacterial growth, displaying type-dependent inhibition effects. The inhibition tendency of Tween 80-stabilized AgNPs at a dose of 1.22 mg/L indicated that they caused almost no bacterial growth or cell death, similar to that observed with pure AgNPs at a concentration of 9.76 mg/L. However, Ag^+ induced an obvious inhibition effect on the bacterial growth at its MIC (1.24 mg/L). 1.22 mg/L of surfactants-stabilized AgNPs, which only contains 0.46 μg/mL of Ag^+, caused better bacteriostatic activity than Ag^+. The phenomenon in our present experiment consists with previous studies, in which Tween 80-stabilized AgNPs display not only stronger bacteriostatic activity but also bactericidal effect.

3.6. Observation of Morphological Changes Using TEM. The important results obtained thus far suggest that the various stabilizers affect the antimicrobial activity of AgNPs differently. Among them, Tween 80 has been found to be the most effective modifier for the improvement of the antibacterial activity of AgNPs. Therefore, in the further study, Tween 80-stabilized AgNPs were selected to investigate the toxicity mechanism.

The initial step in AgNPs antibacterial activity involves contact with the biological samples [42]. The direct contact between biological cells and nanomaterials establishes a series of nanoparticle/biological interfaces, which induce biocompatible or adverse outcomes [43]. Therefore, it is necessary to study the interactions between pathogenic bacteria and AgNPs. The underlying antibacterial mechanism induced through physical contact was examined using TEM to visualize the cell morphology. As shown in Figure 4, the control samples (untreated *R. solanacearum* cells) were observed as integrated cell structures with obvious outer envelopes. However, after incubation with pure AgNPs (19.5 mg/L) at 30°C for 3 h, the bacterial cells displayed morphological changes. The cell membrane became rough, and the cell structure was

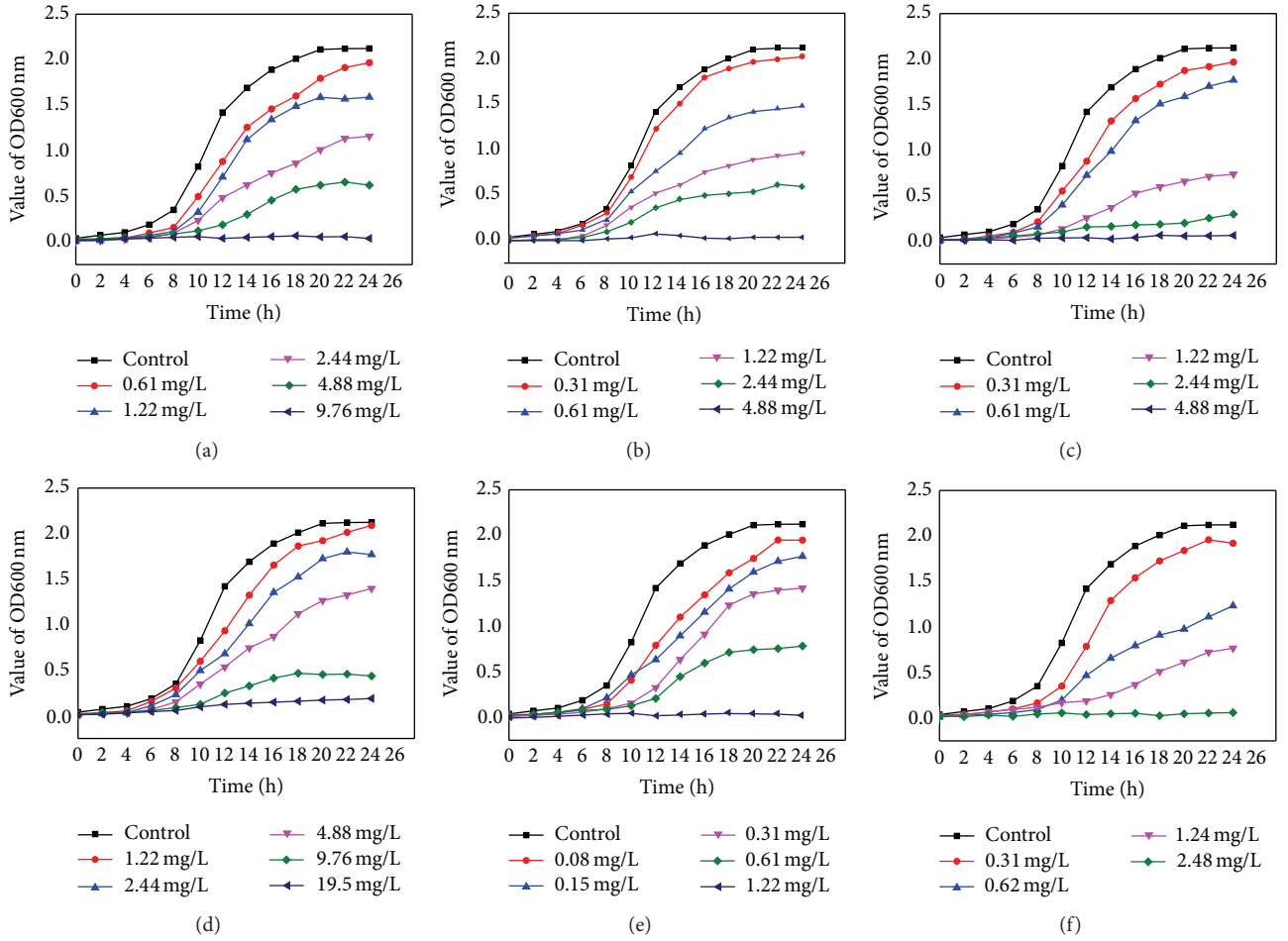

FIGURE 3: Growth kinetics curve of *R. solanacearum* in the presence of different concentrations of pure silver nanoparticles (a) as well as AgNPs stabilized by SDS (b), SDBS (c), TX-100 (d) and Tween 80 (e), and Tween 80 mixed with Ag^+ (f). The concentration of surfactant in stabilized AgNPs is indicated in the form of {AgNPs mg/L (surfactant %)}, such as 19.5 mg/L (0.25%), 9.76 mg/L (0.125%), 4.88 mg/L (6.25×10^{-2}%), 2.44 mg/L (3.125×10^{-2}%), 1.22 mg/L (1.56×10^{-2}%), 0.61 mg/L (0.78×10^{-2}%), and 0.31 mg/L (0.39×10^{-2}%). Similarly, the concentration of surfactant in stabilized-Ag^+ is indicated as 0.31 (0.04×10^{-2}), 0.62 (0.09×10^{-2}), 1.24 (0.19×10^{-2}), and 2.48 (0.39×10^{-2}).

partly hollow, with distortion. In the presence of Tween 80-stabilized AgNPs (1.22 mg/L), much more damage to the *R. solanacearum* cells was observed. As shown in Figure 5(d), the cell structure was looser, and the cytoplasmic density of cells was reduced, likely indicating that the cellular content leaked out during the direct nanoparticle-cell contact, inducing subsequent bacterial growth inhibition and cell death. These observations clearly confirmed that Tween 80 could strongly enhance the antibacterial activity of AgNPs. The particle-cell interface played an essential role in the antibacterial activity of AgNPs [40]. Strong interactions with the cell wall were observed, reflecting the high surface energy and mobility of nanoparticles [40]. Meanwhile, the dilution of Ag^+ from the surface of AgNPs and subsequent attachment to negatively charged bacterial cells is not a negligible antibacterial mechanism [44, 45], as stated in Table 1. Based on a comparison assay, though Tween 80-Ag^+ (2.48 mg/L) also displayed a significant reduction in the bacterial growth in Figure 3, some moderate destructions on the cell membrane were observed in TEM images (Figure 4(d)). Thus, the stabilizer greatly improves the ability of AgNPs to attach to bacterial cells.

3.7. Fluorescence Microscopy Imaging. The results of the present study provide strong evidence that bacteria experience structural changes and cell membrane damage in the presence of Tween 80-stabilized AgNPs. To determine whether AgNPs exhibit strong toxicity to bacteria and verify the reliability of the bactericidal experiment, we conducted experiments using fluorescent dyes, namely, propidium iodide (PI) and 4-6-diamidino-2-phenylindole (DAPI). PI and DAPI are effective imaging tools for the identification of cell membrane damage. Live bacteria cells have intact membranes and are impermeable to PI, which can only enter cells with disrupted membranes. However, DAPI, a membrane-permeable dye, can easily cross the bacterial membrane and combine with DNA in the cell nucleus, emitting blue fluorescence. After treatment with Tween 80-stabilized AgNPs at 1.22 mg/L, the bacteria suspensions were dyed using PI and DAPI, referring to the previous study [46].

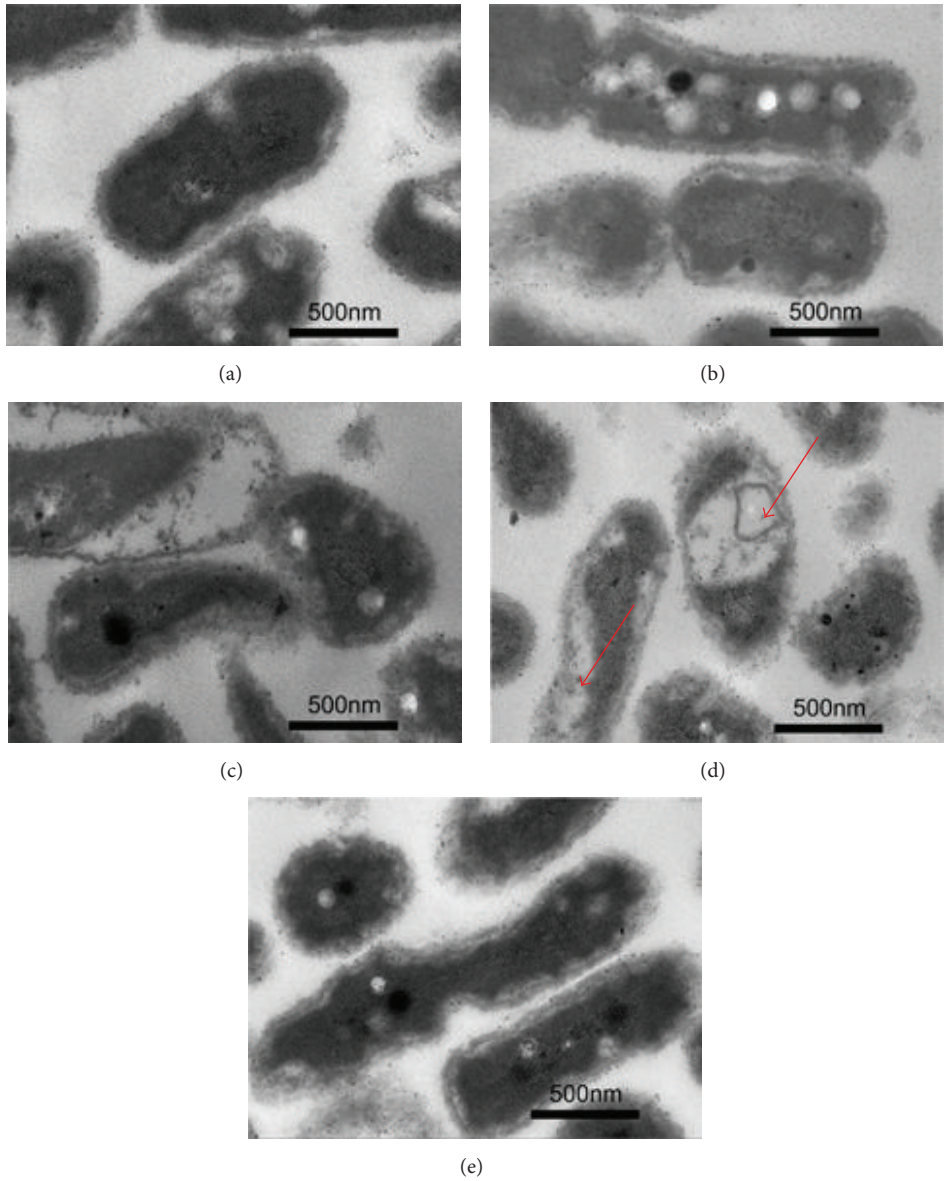

Figure 4: TEM micrographs of *R. solanacearum* cells alone (a) and incubated with 8% (w/w) Tween 80 (b), 19.5 mg/L pure AgNPs (c), 1.22 mg/L Tween 80-stabilized AgNPs (d), and 2.48 mg/L Tween 80-stabilized Ag^+ (e) at 30°C for 3 h with shaking at 120 rpm.

As shown in Figure 5(a), a significant uptake of blue DAPI by untreated *R. solanacearum* cells was clearly observed using a fluorescence microscope (Eclipse Ti, Nikon). However, after counterstaining with red PI, the *R. solanacearum* cells incubated with Tween 80-stabilized AgNPs and Ag^+ primarily displayed red fluorescence as a result of the influx of membrane-impermeable fluorescent PI, indicating that the membrane integrity of the bacteria was disturbed, consistent with the morphologies observed in the TEM imaging studies.

3.8. Protein Damage. We employed SDS-PAGE to determine whether the bacterial proteins were damaged in response to exposure to modified silver nanoparticles. Examining the cytoplasmic proteins is important for determining the effects of nanomaterial exposure, particularly examining the generation of free radicals and reactive oxygen species in biological cells [47]. A previous study investigating the molecular basis of the induced toxicity of some compounds showed that poly(phenylene ethynylene) (PPE) based cationic conjugated polyelectrolytes (CPEs) and oligo-phenylene ethynylenes (OPEs) can exert toxicity on *E. coil* cells, which is strongly associated with the action of ROS, which directly or indirectly covalently modify cytoplasmic biomolecules, such as proteins and DNA [48]. To our knowledge, these studies have shown that the strong toxicity of AgNPs toward bacteria reflects physical and chemical interference involving cell membrane change or permeability induced by AgNPs and the release of silver ions [37, 40]. However, studies have also shown that the generation of free radicals (intracellular ROS) contributes to AgNP-triggered antibacterial activity [49]. Indeed, there is lack of information available regarding the effect of AgNPs (or stabilized AgNPs) on the cellular protein of

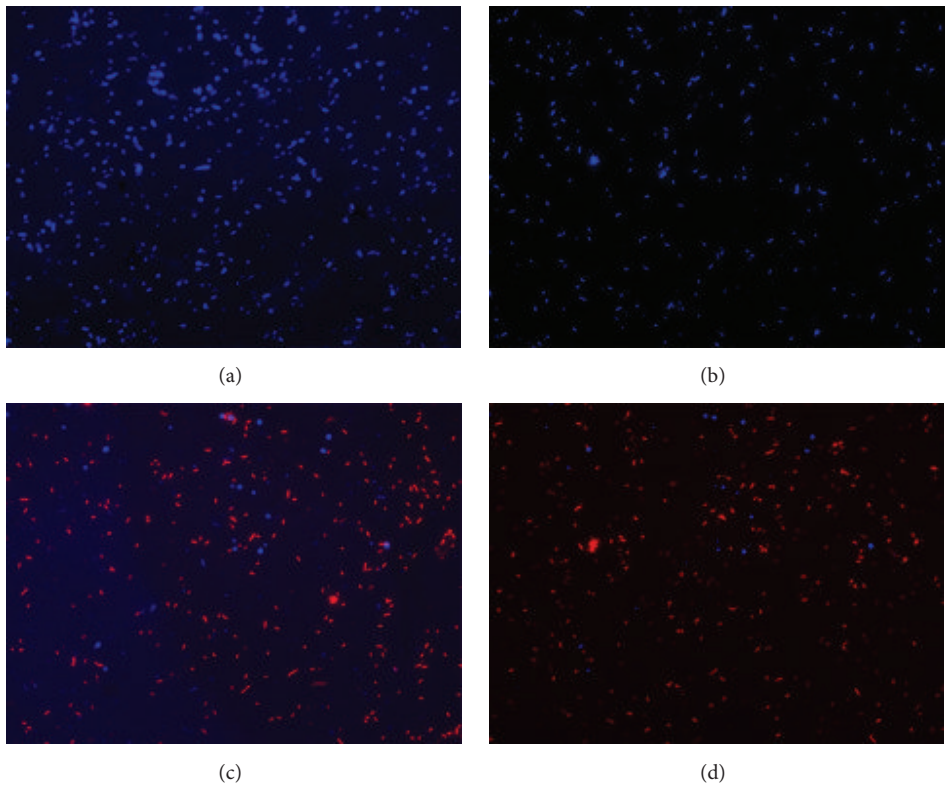

Figure 5: Cell membrane integrity measurements using fluorescence microscopy. Fluorescence imaging of *R. solanacearum* cells incubated with (a) DI water, (b) Tween 80, (c) Tween 80-stabilized (1.22 mg/L), and (d) Tween 80-stabilized Ag^+ (2.48 mg/L) followed by staining with propidium iodide (PI) and DAPI.

phytopathogens. Figure 6 shows a distinct cellular protein response to the presence of various materials. Compared with the control cells, the electrophoretic mobility or band intensity of the proteins from *R. solanacearum* cells treated with Tween 80-stabilized AgNPs was very thin, indicating that the proteins with high molecular weights were largely prevented from entering the electrophoresis gel, reflecting cellular protein modifications and damage likely induced through the binding of some protein fragments with AgNPs. A similar result was observed for Ag^+ mixed with Tween 80, but the protein bands with big molecular weights electrophoretically were slightly heavier than Tween 80-stabilized AgNPs. However, the protein bands from cells incubated with Tween 80 alone were darker than those from cells treated with pure and stabilized AgNPs. This result may reflect the attachment of AgNPs to the cell surface of biomolecules, making these particles more toxic due to the release and diffusion effects of aqueous Ag^+ through the oxidation of the Ag^0 outside the silver nanoparticle [49]. Additionally, after surfactant stabilization, the Ag nanoparticles might have more opportunities to contact *R. solanacearum* cells than do pure AgNPs. It has been suggested that DNA loses replication ability and cellular proteins become inactivated after Ag^+ treatment [48]. In addition, studies have shown that Ag^+ binds to the functional groups of proteins, resulting in protein denaturation [10]. From the above results, it can be stated that Tween 80-stabilized AgNPs seem to exhibit stronger toxicity on *R. solanacearum* than Ag^+. This stabilization by Tween 80 blocks the aggregation of AgNPs nanoparticles, thus improving the opportunities of nanoparticles to contact with bacterial cells, facilitating the implementation of their antimicrobial properties. Hence, the control efficacy of the materials on bacterial wilt *in vivo* is investigated in the following research.

3.9. Efficacy of Tween-Stabilized AgNPs on Controlling of Tobacco Bacterial Wilt. The high effectiveness of Tween-stabilized AgNPs on tobacco bacterial wilt at 1.22 mg/L was performed by the pot experiment. The disease index and control efficacy at 7 days, 14 days, and 21 days after Tween 80-stabilized AgNPs irrigation of tobacco roots were investigated, respectively. From Table 2, it was found that application of AgNPs can significantly prevent the incidence of bacterial wilt disease on tobacco compared to the untreated plant. In the presence of Tween 80-stabilized AgNPs, the control efficacies were 96.71%, 90.11%, and 84.21% after inoculation with *R. solanacearum*, respectively. The disease index is 8.21% at 21 days of irrigating, which is reduced by 91.79%, compared to the value of 100% in the control treatment.

The present study presented a detailed and systematic examination of the effect of surfactants on the antibacterial activity of silver nanoparticles against pathogenic bacteria *in vitro* and *in vivo*. Tween 80, as a nonionic stabilizer, showed biocompatibility and a moderate antibacterial effect, even at the highest concentration (8% w/w) (Figure S2). Considering the gentleness of Tween 80, this surfactant was the best

Table 2: The disease index and control efficacy of Tween 80-stabilized AgNPs on tobacco bacterial wilt.

Treatments	7 days after irrigating		14 days after irrigating		21 days after irrigating	
	Disease index (%)	Control efficiency (%)	Disease index (%)	Control efficiency (%)	Disease index (%)	Control efficiency (%)
CK	61.24	—	84.23	—	100	—
Tween 80-stabilized AgNPs	5.71	96.71	6.56	90.11	8.21	84.21

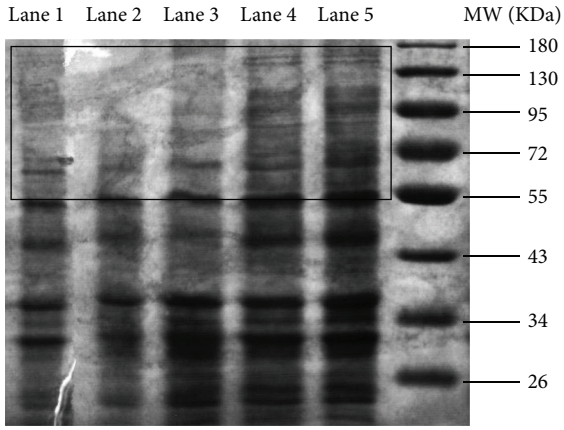

Figure 6: SDS-PAGE gels analysis of the protein samples obtained from *R. solanacearum* cells treated with Tween 80-stabilized Ag^+ (Lane 1), Tween 80-stabilized AgNPs (Lane 2), pure AgNPs (Lane 3), Tween 80 (Lane 4), and DI water (Lane 5). *R. solanacearum* cells were grown at 30°C to the exponential phase in NB medium and subsequently incubated with Tween 80, 19.5 mg/L AgNPs, 1.22 mg/L Tween 80-stabilized AgNPs, or 2.48 mg/L Tween 80-stabilized Ag^+ for 2 h, followed by SDS-PAGE.

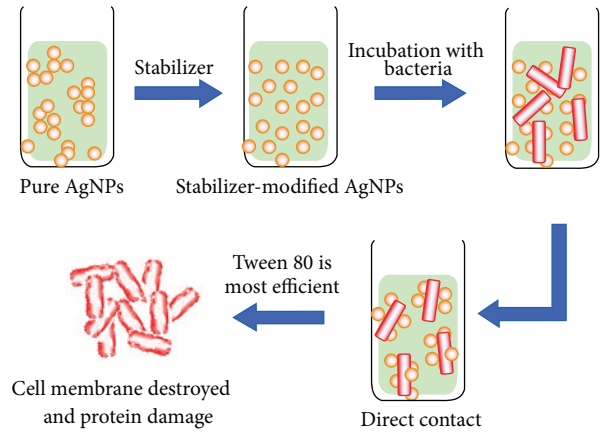

Figure 7: Schematic illustration of the surfactant-mediated stabilization and antibacterial characteristics of AgNPs against the phytopathogenic bacterium *R. solanacearum*.

candidate for stabilizing AgNPs for further application as excellent antimicrobial agents. These experimental results showed that, among the four solutions, Tween 80 displayed a remarkable stabilizing effect, which is connected with the steric stabilization effect, with a considerable enhancement of the silver NP stability compared with the unmodified sample. Interestingly, previous studies have shown that the antibacterial activity of AgNPs toward *E. coli* and *S. aureus* in the presence of the nonionic surfactant Tween 80 was lower than that observed with SDS and CTAB [31], whereas the contrary result was observed for *Pseudomonas aeruginosa*, consistent with the results obtained in the present study. Moreover, another study showed that SDS-stabilized AgNPs did not display enhanced antibacterial activity [50]. It is therefore likely that various surfactants influence the toxicity of AgNPs differently, likely reflecting the effects of the synthesis conditions, bacteria strain, bacterial concentration, and so forth. However, for *R. solanacearum*, Tween 80 is the best tool for improving the toxicity of AgNPs, although this surfactant was not the best stabilizer. And Tween 80-stabilized AgNPs can completely kill the bacteria at low concentration of 1.22 mg/L. The enhancement of dispersibility increased the specific surface area and probability for interactions with biological cells, resulting in a loss of cell activity and damage to the cell proteins, as indicated in Figure 7.

Notably, in the present study, a distinctly synergic antibacterial effect was observed for SDS- and SDBS-stabilized AgNPs (Table 1), increasing the inactivation of bacteria cells. Anionic SDS interacts strongly with proteins on the surface of the cell membranes, particularly Gram-positive bacteria, through electrostatic interactions, reflecting the high surface energy and mobility of this detergent [51], thus facilitating the interaction of Ag nanoparticles with cells. This observation was consistent with the results of a previous study showing that the activity of a mixture of methionine and riboflavin for controlling powdery mildew infection was improved after supplementation with SDS [52]. However, *in vitro* antibacterial studies of modified AgNPs showed that Tween 80 could enhance the dispersibility of silver nanoparticles as an effective performance enhancer of the toxicity of AgNPs, suggesting the potential of this surfactant as an antibacterial adjuvant of AgNPs for protecting crops from disease.

In consequence, evaluation of the control efficacy of Tween-stabilized AgNPs was further performed in the present study. It is found that Tween 80-stabilized AgNPs are also an effective antibacterial agent against tobacco bacterial wilt *in vivo*. The control efficacies on bacterial wilt disease are 96.71%, 90.11%, and 84.21%, respectively, after irrigating tobacco roots. Most importantly, such an application in agriculture for controlling plant disease using antimicrobials has previously been discussed in other studies [18, 24, 25], although the nanotoxicity of AgNPs has previously been recognized toward various biology samples. According to

USEPA guidelines, nanomaterials only exhibit minimal toxicity on plants at a high concentration of 2000 mg/L (USEPA, 1996) [53]. One of the key results of the present study is the high antibacterial activity and control effectiveness of Tween 80-modified AgNPs at a low dose of 1.22 mg/L on *R. solanacearum in vitro* and *in vivo*, displaying the superiority application prospects of these particles as alternative antibacterial agents for controlling tobacco bacterial wilt. In future studies, we will analyze plant growth patterns upon exposure to different AgNPs concentrations to provide information about the phytotoxicology of nanoparticles.

4. Conclusions

The aim of the present study was to identify an available strategy for improving the antibacterial activity and reducing the usage concentration of AgNPs. Herein, we compared and discussed the antibacterial action of pure and stabilized AgNPs in the presence of four surfactants (SDS, SDBS, TX-100, and Tween 80) toward the phytopathogenic bacterium *Ralstonia solanacearum*, which causes destructive bacterial wilt disease. The results indicated that all of the surfactants favored the dispersion of pure AgNPs, and surfactant-stabilized AgNPs displayed much higher toxicity. Among the surfactants examined, Tween 80 was the most appropriate for stabilizing AgNPs because of its biocompatibility; even the antibacterial activity of Tween 80-stabilized AgNPs is superior to silver ion in the presence of surfactants. The MIC and MBC of surfactant-stabilized AgNPs were found to be much lower than those obtained for pure AgNPs, except in the case of TX-100. Further fluorescence and TEM imaging demonstrated that outer cell membrane disruption is an important toxicity mechanism. The interaction between nanoparticles and bacterial pathogens is also responsible for the cellular protein damage induced by AgNPs. For *in vivo* application, the control efficacy of Tween-stabilized AgNPs still reached 84.21% after 21 days of irrigating. Taken together, these results demonstrated that Tween 80-stabilized AgNPs have great potential as biocides for managing plant disease.

Competing Interests

The authors declare they have no competing interests.

Authors' Contributions

Juanni Chen designed the experiment and performed the synthesis of silver nanoparticles (AgNPs) and the pot experiment. Shili Li performed the characterization by TEM and so on. Jinxiang Luo carried out the antibacterial activity of AgNPs and the mechanism using TEM. Rongsheng Wang did the fluorescence microscopy and SDS-PAGE experiment. Juanni Chen and Shili Li wrote the paper. Wei Ding supervised the project. All authors discussed the results and commented on the paper and all authors read and approved the final paper.

Acknowledgments

This work was financially supported through grants from the Chongqing Postdoctoral Science Foundation (Xm2015129), National Natural Science Foundation of China (31272058), the Fundamental Research Funds for the Central Universities (2120132349), the Key Project of the State Tobacco Monopoly Administration (NY20130501070005), and the Key Project of the Chongqing Tobacco Monopoly Administration (110201202002). One of the authors would like to express great gratitude to all those who helped in finishing the supplement experiments, including Long Sun, Lin Cai, and Zhiyu Lin.

References

[1] V. Grimault, G. Anais, and P. Prior, "Distribution of *Pseudomonas solanacearum* in the stem tissues of tomato plants with different levels of resistance to bacterial wilt," *Plant Pathology*, vol. 43, no. 4, pp. 663–668, 1994.

[2] A. C. Hayward, "Biology and epidemiology of bacterial wilt caused by *Pseudomonas solanacearum*," *Annual Review of Phytopathology*, vol. 29, pp. 65–87, 1991.

[3] I. Buddenhagen and A. Kelman, "Biological and physiological aspects of bacterial wilt caused by *Pseudomonas solanacearum*," *Annual Review of Phytopathology*, vol. 2, no. 1, pp. 203–230, 1964.

[4] E. Saile, J. A. McGarvey, M. A. Schell, and T. P. Denny, "Role of extracellular polysaccharide and endoglucanase in root invasion and colonization of tomato plants by Ralstonia solanacearum," *Phytopathology*, vol. 87, no. 12, pp. 1264–1271, 1997.

[5] P. Thoquet, J. Olivier, C. Sperisen, P. Rogowsky, H. Laterrot, and N. Grimsley, "Quantitative trait loci determining resistance to bacterial wilt in tomato cultivar Hawaii7996," *Molecular Plant-Microbe Interactions*, vol. 9, no. 9, pp. 826–836, 1996.

[6] L. Deslandes, J. Olivier, F. Theulières et al., "Resistance to *Ralstonia solanacearum* in *Arabidopsis thaliana* is conferred by the recessive RRS1-R gene, a member of a novel family of resistance genes," *Proceedings of the National Academy of Sciences of the United States of America*, vol. 99, no. 4, pp. 2404–2409, 2002.

[7] D. R. Fravel, "Role of antibiosis in the biocontrol of plant diseases," *Annual Review of Phytopathology*, vol. 26, no. 1, pp. 75–91, 1988.

[8] J. C. Wynne, M. K. Beute, and S. N. Nigam, "Breeding for disease resistance in peanut (*Arachis Hypogaea* L.)," *Annual Review of Phytopathology*, vol. 29, no. 1, pp. 279–303, 1991.

[9] H. Chen and R. Yada, "Nanotechnologies in agriculture: new tools for sustainable development," *Trends in Food Science and Technology*, vol. 22, no. 11, pp. 585–594, 2011.

[10] S. Agnihotri, S. Mukherji, and S. Mukherji, "Size-controlled silver nanoparticles synthesized over the range 5-100 nm using the same protocol and their antibacterial efficacy," *RSC Advances*, vol. 4, no. 8, pp. 3974–3983, 2014.

[11] K. M. Paknikar, V. Nagpal, A. V. Pethkar, and J. M. Rajwade, "Degradation of lindane from aqueous solutions using iron sulfide nanoparticles stabilized by biopolymers," *Science and Technology of Advanced Materials*, vol. 6, no. 3-4, pp. 370–374, 2005.

[12] T. K. Barik, B. Sahu, and V. Swain, "Nanosilica—from medicine to pest control," *Parasitology Research*, vol. 103, no. 2, pp. 253–258, 2008.

[13] M. Lisa, R. S. Chouhan, A. C. Vinayaka, H. K. Manonmani, and M. S. Thakur, "Gold nanoparticles based dipstick immunoassay for the rapid detection of dichlorodiphenyltrichloroethane: an organochlorine pesticide," *Biosensors and Bioelectronics*, vol. 25, no. 1, pp. 224–227, 2009.

[14] K. S. Yao, S. J. Li, K. C. Tzeng et al., "Fluorescence silica nanoprobe as a biomarker for rapid detection of plant pathogens," *Advanced Materials Research*, vol. 79–82, pp. 513–516, 2009.

[15] A. Manceau, K. L. Nagy, M. A. Marcus et al., "Formation of metallic copper nanoparticles at the soil-root interface," *Environmental Science and Technology*, vol. 42, no. 5, pp. 1766–1772, 2008.

[16] J. R. Morones, J. L. Elechiguerra, A. Camacho et al., "The bactericidal effect of silver nanoparticles," *Nanotechnology*, vol. 16, no. 10, pp. 2346–2353, 2005.

[17] A. Panáček, M. Kolář, R. Večeřová et al., "Antifungal activity of silver nanoparticles against *Candida* spp.," *Biomaterials*, vol. 30, no. 31, pp. 6333–6340, 2009.

[18] S. W. Kim, J. H. Jung, K. Lamsal, Y. S. Kim, J. S. Min, and Y. S. Lee, "Antifungal effects of silver nanoparticles (AgNPs) against various plant pathogenic fungi," *Mycobiology*, vol. 40, no. 1, pp. 53–58, 2012.

[19] C. Marambio-Jones and E. M. V. Hoek, "A review of the antibacterial effects of silver nanomaterials and potential implications for human health and the environment," *Journal of Nanoparticle Research*, vol. 12, no. 5, pp. 1531–1551, 2010.

[20] J. Thiel, L. Pakstis, S. Buzby et al., "Antibacterial properties of silver-doped titania," *Small*, vol. 3, no. 5, pp. 799–803, 2007.

[21] G. A. Martinez-Castanon, N. Niño-Martínez, F. Martínez-Gutierrez, J. R. Martínez-Mendoza, and F. Ruiz, "Synthesis and antibacterial activity of silver nanoparticles with different sizes," *Journal of Nanoparticle Research*, vol. 10, no. 8, pp. 1343–1348, 2008.

[22] G. A. Sotiriou, A. Meyer, J. T. N. Knijnenburg, S. Panke, and S. E. Pratsinis, "Quantifying the origin of released Ag^+ ions from nanosilver," *Langmuir*, vol. 28, no. 45, pp. 15929–15936, 2012.

[23] P. Zhang, H. Cui, X. Zhong, and L. Li, "Effects of nano—TiO_2 semiconductor sol on prevention from plant diseases," *Nanoscience*, vol. 12, no. 1, pp. 1–6, 2007.

[24] Y.-K. Jo, B. H. Kim, and G. Jung, "Antifungal activity of silver ions and nanoparticles on phytopathogenic fungi," *Plant Disease*, vol. 93, no. 10, pp. 1037–1043, 2009.

[25] K. Lamsal, S.-W. Kim, J. H. Jung, Y. S. Kim, K. S. Kim, and Y. S. Lee, "Inhibition effects of silver nanoparticles against powdery mildews on cucumber and pumpkin," *Mycobiology*, vol. 39, no. 1, pp. 26–32, 2011.

[26] S. M. Ouda, "Antifungal activity of silver and copper nanoparticles on two plant pathogens, Alternaria alternata and Botrytis cinerea," *Research Journal of Microbiology*, vol. 9, no. 1, pp. 34–42, 2014.

[27] M. Chen, L.-Y. Wang, J.-T. Han, J.-Y. Zhang, Z.-Y. Li, and D.-J. Qian, "Preparation and study of polyacryamide-stabilized silver nanoparticles through a one-pot process," *The Journal of Physical Chemistry B*, vol. 110, no. 23, pp. 11224–11231, 2006.

[28] M. Lv, S. Su, Y. He et al., "Long-term antimicrobial effect of silicon nanowires decorated with silver nanoparticles," *Advanced Materials*, vol. 22, no. 48, pp. 5463–5467, 2010.

[29] J. Tang, Q. Chen, L. Xu et al., "Graphene oxide-silver nanocomposite as a highly effective antibacterial agent with species-specific mechanisms," *ACS Applied Materials and Interfaces*, vol. 5, no. 9, pp. 3867–3874, 2013.

[30] S. Pal, Y. K. Tak, and J. M. Song, "Does the antibacterial activity of silver nanoparticles depend on the shape of the nanoparticle? A study of the gram-negative bacterium *Escherichia coli*," *Applied and Environmental Microbiology*, vol. 73, no. 6, pp. 1712–1720, 2007.

[31] L. Kvítek, A. Panáček, J. Soukupová et al., "Effect of surfactants and polymers on stability and antibacterial activity of silver nanoparticles (NPs)," *The Journal of Physical Chemistry C*, vol. 112, no. 15, pp. 5825–5834, 2008.

[32] Y. Xiong, M. Brunson, J. Huh et al., "The role of surface chemistry on the toxicity of Ag nanoparticles," *Small*, vol. 9, no. 15, pp. 2628–2638, 2013.

[33] P. C. Lee and D. Meisel, "Adsorption and surface-enhanced Raman of dyes on silver and gold sols," *The Journal of Physical Chemistry*, vol. 86, no. 17, pp. 3391–3395, 1982.

[34] J. Yang, Q. Zhang, J. Y. Lee, and H.-P. Too, "Dissolution-recrystallization mechanism for the conversion of silver nanospheres to triangular nanoplates," *Journal of Colloid and Interface Science*, vol. 308, no. 1, pp. 157–161, 2007.

[35] X. A. Li, J. J. Lenhart, and H. W. Walker, "Dissolution-accompanied aggregation kinetics of silver nanoparticles," *Langmuir*, vol. 26, no. 22, pp. 16690–16698, 2010.

[36] M. Chen, L.-Y. Wang, J.-T. Han, J.-Y. Zhang, Z.-Y. Li, and D.-J. Qian, "Preparation and study of polyacryamide-stabilized silver nanoparticles through a one-pot process," *Journal of Physical Chemistry B*, vol. 110, no. 23, pp. 11224–11231, 2006.

[37] P. Pallavicini, A. Taglietti, G. Dacarro et al., "Self-assembled monolayers of silver nanoparticles firmly grafted on glass surfaces: low Ag^+ release for an efficient antibacterial activity," *Journal of Colloid and Interface Science*, vol. 350, no. 1, pp. 110–116, 2010.

[38] A. M. El Badawy, T. P. Luxton, R. G. Silva, K. G. Scheckel, M. T. Suidan, and T. M. Tolaymat, "Impact of environmental conditions (pH, ionic strength, and electrolyte type) on the surface charge and aggregation of silver nanoparticles suspensions," *Environmental Science and Technology*, vol. 44, no. 4, pp. 1260–1266, 2010.

[39] X. Li, J. J. Lenhart, and H. W. Walker, "Aggregation kinetics and dissolution of coated silver nanoparticles," *Langmuir*, vol. 28, no. 2, pp. 1095–1104, 2012.

[40] A. Taglietti, Y. A. Diaz Fernandez, E. Amato et al., "Antibacterial activity of glutathione-coated silver nanoparticles against gram positive and gram negative bacteria," *Langmuir*, vol. 28, no. 21, pp. 8140–8148, 2012.

[41] Y.-H. Chen and C.-S. Yeh, "Laser ablation method: use of surfactants to form the dispersed Ag nanoparticles," *Colloids and Surfaces A: Physicochemical and Engineering Aspects*, vol. 197, no. 1–3, pp. 133–139, 2002.

[42] O. Bondarenko, A. Ivask, A. Käkinen, I. Kurvet, and A. Kahru, "Particle-cell contact enhances antibacterial activity of silver nanoparticles," *PLoS ONE*, vol. 8, no. 5, Article ID e64060, 2013.

[43] A. E. Nel, L. Mädler, D. Velegol et al., "Understanding biophysicochemical interactions at the nano-bio interface," *Nature Materials*, vol. 8, no. 7, pp. 543–557, 2009.

[44] W. K. Jung, H. C. Koo, K. W. Kim, S. Shin, S. H. Kim, and Y. H. Park, "Antibacterial activity and mechanism of action of the silver ion in *Staphylococcus aureus* and *Escherichia coli*," *Applied*

and Environmental Microbiology, vol. 74, no. 7, pp. 2171–2178, 2008.

[45] Z.-M. Xiu, J. Ma, and P. J. J. Alvarez, "Differential effect of common ligands and molecular oxygen on antimicrobial activity of silver nanoparticles versus silver ions," *Environmental Science and Technology*, vol. 45, no. 20, pp. 9003–9008, 2011.

[46] J. Chen, H. Peng, X. Wang, F. Shao, Z. Yuan, and H. Han, "Graphene oxide exhibits broad-spectrum antimicrobial activity against bacterial phytopathogens and fungal conidia by intertwining and membrane perturbation," *Nanoscale*, vol. 6, no. 3, pp. 1879–1889, 2014.

[47] Y. Li, W. Zhang, J. Niu, and Y. Chen, "Mechanism of photogenerated reactive oxygen species and correlation with the antibacterial properties of engineered metal-oxide nanoparticles," *ACS Nano*, vol. 6, no. 6, pp. 5164–5173, 2012.

[48] Y. Wang, S. D. Jett, J. Crum, K. S. Schanze, E. Y. Chi, and D. G. Whitten, "Understanding the dark and light-enhanced bactericidal action of cationic conjugated polyelectrolytes and oligomers," *Langmuir*, vol. 29, no. 2, pp. 781–792, 2013.

[49] H.-L. Su, C.-C. Chou, D.-J. Hung et al., "The disruption of bacterial membrane integrity through ROS generation induced by nanohybrids of silver and clay," *Biomaterials*, vol. 30, no. 30, pp. 5979–5987, 2009.

[50] E. Bae, H.-J. Park, J. Park et al., "Effect of chemical stabilizers in silver nanoparticle suspensions on nanotoxicity," *Bulletin of the Korean Chemical Society*, vol. 32, no. 2, pp. 613–619, 2011.

[51] K.-H. Cho, J.-E. Park, T. Osaka, and S.-G. Park, "The study of antimicrobial activity and preservative effects of nanosilver ingredient," *Electrochimica Acta*, vol. 51, no. 5, pp. 956–960, 2005.

[52] S. Y. Wang and D. D.-S. Tzeng, "Methionine-riboflavin mixtures with surfactants and metal ions reduce powdery mildew infection in strawberry plants," *Journal of the American Society for Horticultural Science*, vol. 123, no. 6, pp. 987–991, 1998.

[53] U.S. Envionmental Protection Agency, *Nanotechnology White Paper External Review Draft*, 2005, http://nepis.epa.gov/Exe/ZyNET.exe/60000EHU.TXT?ZyActionD=ZyDocument&Client=EPA&Index=2006+Thru+2010&Docs=&Query=&Time=&EndTime=&SearchMethod=1&TocRestrict=n&Toc=&TocEntry=&QField=&QFieldYear=&QFieldMonth=&QFieldDay=&IntQFieldOp=0&ExtQFieldOp=0&XmlQuery=&File=D%3A%5Czyfiles%5CIndex%20Data%5C06thru10%5CTxt%5C00000000%5C60000EHU.txt&User=ANONYMOUS&Password=anonymous&SortMethod=h%7C-&MaximumDocuments=1&FuzzyDegree=0&ImageQuality=r75g8/r75g8/x150y150g16/i425&Display=p%7Cf&DefSeekPage=x&SearchBack=ZyActionL&Back=ZyActionS&BackDesc=Results%20page&MaximumPages=1&ZyEntry=1&SeekPage=x&ZyPURL.